Steel and Composite Structures, Vol. 3, No. 2 (2003) 123-140
DOI: http://dx.doi.org/10.12989/scs.2003.3.2.123

Flexural behavior and resistance of uni-planar KK and X tubular joints

Yiyi Chen† and Wei Wang‡

Department of Building Engineering, Tongji University, Shanghai 200092, China

(Received April 15, 2002, Accepted March 25, 2003)

Abstract. The importance of the research on moment-resistant properties of unstiffened tubular joints and the research background are introduced. The performed experimental research on the bending rigidity and capacity of the joints is reported. The emphasis is put on the discussion of the flexural behavior of the joints including sets of geometrical parameters of the joints and several loading combinations. Procedures and results of loading tests on four full size joints in planar KK and X configuration are described in details at first. Mechanical models are proposed to analyze the joint specimens. Three-dimensional nonlinear FE models are established and verified with the experimental results. By comparing the experimental data with the results of the analysis, it is reported reasonable to carry out the structural analysis under the assumption that the joint is fully rigidly connected, and their bending capacities can assure the strength of the members connected under certain limitation. Furthermore, a parametric formula for inplane bengding rigidity of T and Y type tubular joints is proposed on the basis of FE calculation and regression analysis. Compared with test results, it is shown that the parametric formula developed in this paper has good applicability.

Key words: unstiffened tubular joint; flexural behavior; bending rigidity; loading test; non-linear FE analysis; joint rigidity evaluation.

1. Introduction

By the late 1950s, many steel mills all over the world had begun to produce hollow structural sections (HSS), as their excellent properties suitable for building structures were recognized. One of the most popular applications of circular hollow section (CHS) to architectural structures, is welded tubular trusses or reticulated shells, most often in a warren ("*K*" connection) or Pratt ("*N*" connection) configuration. The tubular members are normally joined together by unstiffened joint which connects the carefully contoured ends of the brace members to the continuous chord by penetrated or fillet welds. This kind of joint requires no additional connecting elements, makes materials saving, and is with high load-bearing capacity. Because of these merits, there has been an ever increasing use of this joint type in steel-tube structures.

Since 1950, researchers have carried out a large amount of experimental and theoretical analyses on the structural behavior of unstiffened tubular joints. Most of this research focused on issues such as the determination of static strength (Yura and Zettlemoyer 1981, Kurobane and Makino *et al.* 1984,

†Professor
‡Graduate student

Wardenier *et al.* 1991), the evaluation of stress concentration factors (Gibstein 1987) and also the fatigue bebaviour (Soh *et al.* 1993, Moffat *et al.* 1991). Main research achievements have been introduced into the designing specifications or handbooks. However, those research work are mainly limited to the field of bearing capacity, rarely dealing with the rigidity of the joint zone.

The conventional procedure for the design and analysis of offshore structures is to assume that the joints are completely rigid (Rodabaugh 1980). In other words, it is supposed that no local distortion of the chords in circular cross-section occurs and hence there are no tilt, compressive or tensile deformation in the direction of brace members within the joint zone of chord member. As a matter of fact, most unstiffened tubular joins are not completely rigid and the loaded braces always cause local distortion of the chord cross-section. Recent research has indicated that the inclusion of the finite joint stiffness in a structural analysis yields markedly different member actions from those results acquired by conventional rigid-joint model. By numerical analysis performed by Holmas (1987), bending-moments of certain members in a jacket structure changed approximately 100 percent, while other structural actions and other structural members were affected to a smaller but still significant extent. Tests by other authors have led to similar conclusions. In the field of theoretical study, results from limited analytical studies using a modified three-dimensional finite element formulation have indicated that the effects of tubular joint rigidity for towers taller than 350 feet may be significant (Bouwkamp 1980).

On the other side, in the large-span truss structures, the members between joints are usually supposed as pin-connected, permitting a remarkable simplification in the designing procedures. The designer can acquire the analyzing results with tolerable errors in the view of engineering. However, in such a case that a monolayer reticulated shell structure composed of tube members is designed, for example, the engineers have to consider the rigidity of the joint. If there is no enough flexural rigidity, the structure will not be a statically determinate one.

Besides that special case, proper assessment of the local joint rigidity concerns whether the eigenvalue of a tubular structure can be estimated more accurately, how the effective length of compressive members can be determined reasonably, and whether the stress distribution computed is close to the real situation.

In the last few years, some attention has been paid to the local rigidity of unstiffened tubular joints. Mang *et al.* proposed a method to estimate the stiffness of unreinforced T moment RHS joints (Szlendak and Brodka 1985). Fessler and Spooner (1981) tested 25 Araldite model tubular joints, including seven multi-brace joints and derived parametric equations for the flexibility matrices of single brace joints. This was the only published previous work in which the cross-flexibilities between two braces at a point had been measured. Ure (1993) presented a method of determining local joint flexibility of flattened-ended tubular connections using finite element modeling. Japanese researchers (Ogawa *et al.* 1987) produced an out-of-plane rigidity equation of tubular joints. A calculating formula for effective length out-of-plane based on the research was then developed. CIDECT (Rondal 1990) also put forward an equation on this subject.

As mentioned above, the local joint rigidity involves both the capability to resist the flexural distortion and to the even deformation toward the axis of chord. In this paper, the authors report their research work on the former issue. The procedures and results of tests on two uni-planar KK joints and two X joints are first detailed. Analytical models called rigidly connected model and rigid field model in order to ascertain the stiffness are explained briefly. By comparing test results with numerical analysis, the elastic bending rigidity of the joint is appraised. Next the established FE model along with the validation of the model against the experimental results are described. Finally, a parametric formula for local rigidity of T and Y type tubular joints is proposed on the basis of FE calculation and regression analysis.

2. Engineering background of the research

Though unstiffened tubular joints do have certain bending rigidity, the commonly simplified pin-joint analysis satisfies the needs of most design work for architectural structures. Thus when a monolayer reticulated cylindrical shell structure for a new airport terminal was designed, how to determine the joint rigidity of unstiffened tubular joints became an unavoidable problem. By the experience of researchers and engineers, the geometrical parameters of the steel pipes were therefore carefully chosen, so that the joint could behave rigid enough. At the same time, the laboratory experiment and numerical analysis were planed to confirm the predicted stiffness of the joint. However, the researchers covered more comprehensive tasks in the work, not only to investigate whether the determined joint geometry meet the requirements or not, but also to study the parameters which affect the joint stiffness and to find a way to assess the stiffness. Based on such a background, the research was organized in the following steps:

- to structure a flexible test system including loading device and surveying method to obtain the necessary data of the joint stiffness reasonably and reliably.
- to investigate the full scale unstiffened tubular joint specimens which match with the prototype in main geometrical configuration.
- to establish simple analytical model and fine FE shell model in order to found a base for further parametric research.

3. Experiments

3.1. Basic method

There are two different ways in investigating the local joint rigidity: direct method and indirect method. The former is to determine the joint bending rigidity by surveying the bending moment and the relative rotation, which are defined as the changes of the included angle between the axes of the chord and the brace. However, it is difficult to survey the moments directly. In addition, in order to acquire the relative rotation, the rotation induced by member deformation must be deducted from the surveyed value. The basic idea of the latter method is to obtain the curves of lateral forces on the brace ends and the corresponding displacements, thus the rigidity can be estimated by comparison with the results of theoretical analysis.

Indirect method has been widely used in the tests of the beam-to-column connections of steel frame and is also adopted herein.

3.2. Specimens

Since the joint rigidity is closely related to the geometrical parameters of section, the experimental research was carried out on four full-scale tubular joints. Two of them, named DKL and DKS respectively, have KK configuration and the other two, named SXN and SXR respectly, have X configuration. The typical KK joint of the prototype is near to uni-planar joint though the braces connected are slowly curved as shown in Fig. 1. The two uni-planar X joints are shown in Fig. 2. The difference between SXN and SXR is that SXR has stiffeners welded on it. The doughnut like stiffeners, with the size of 12×30 mm, are welded around the outside of the chord wall, 20 mm away from the edge of the brace.

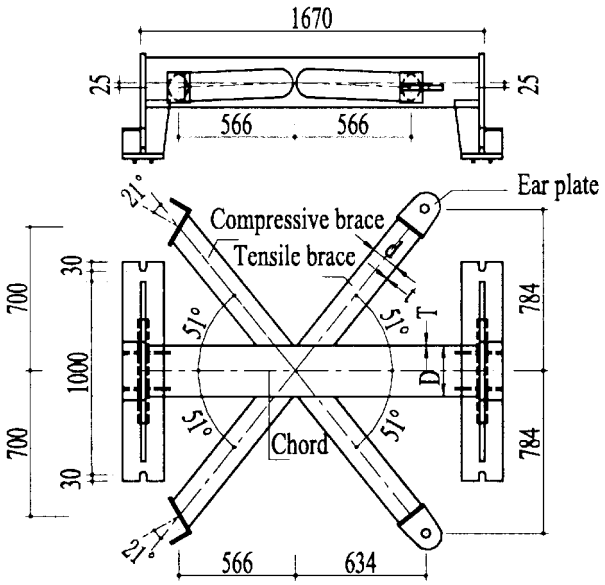

Fig. 1 Specimen DKL and DKS

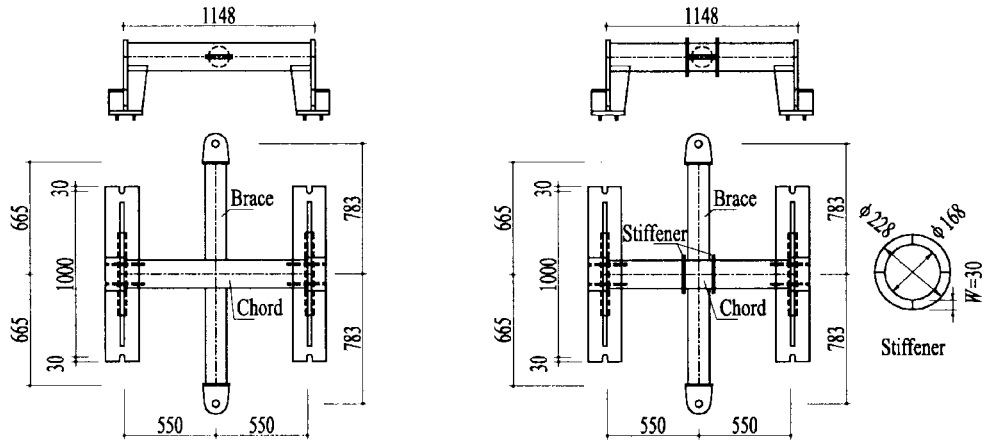

Fig. 2 Specimen SXN and SXR

The geometrical characteristics and details of the test specimens are listed in Table 1. Where, D, T, d, t refer to the diameter, the wall thickness of chord and those of brace respectively, and a to the gap between two braces in the interface of the chord. The geometrical details are in accordance with limitations of designing specifications. The ratio of the diameter to the wall thickness of the chord is given the minimun value within the range of the actual structure. Thick cover plates are welded on each ends of the chord and brace members so that the compressive loads can be applied on uniformly. Ear plates welded on the ends of tensile braces will be connected to the tensile bars which will transfer tension to the test specimen.

Mechanical properties of the steel pipes obtained from tensile coupons are listed in Table 2. Where, f_y,

Table 1 Geometrical characteristics of specimen

Specimen	Chord *D-T* (mm)	Brace *d-t* (mm)	*D/T*	*d/t*	*d/D*	*t/T*	*a/T*	Angle between chord and brace
DKL	245-18	140-8	13.6	17.5	0.57	0.44	1.00	51°
DKS	168-12	127-8	14.0	15.9	0.76	0.67	-2.29	51°
SXN	168-12	127-8	14.0	15.9	0.76	0.67	-	90°
SXR	168-12	127-8	14.0	15.9	0.76	0.67	-	90°

Table 2 Mechanical properties of the steels used in the specimen (Average)

Pipe size (mm)	f_y (N/mm^2)	f_u (N/mm^2)	δ (%)	f_y/f_u
245-18	312	473	28	0.66
168-12	359	465	29	0.77
140-8	324	476	29	0.68
127-8	325	458	28	0.71

f_u are refered to the yield stress and tensile strength, δ to the prolongation of tensile coupons.

3.3. Loading equipments

To execute the loading tests on different types of tubular joint, a planar self-balanced reaction frame as shown in Fig. 3 is designed. The frame is made up of two frame beams and two tensile rods. In the frame beam on the right side four ear plates are welded, through which rigid tensile bars can connect the braces of specimen, thus the tensile force in varying directions can be applied. The beam on the left side is equipped with two triangular bearing supports, which was able to be removed easily, and if the declined angle of the bearer is changed, the compressive loads can change the direction with ease.

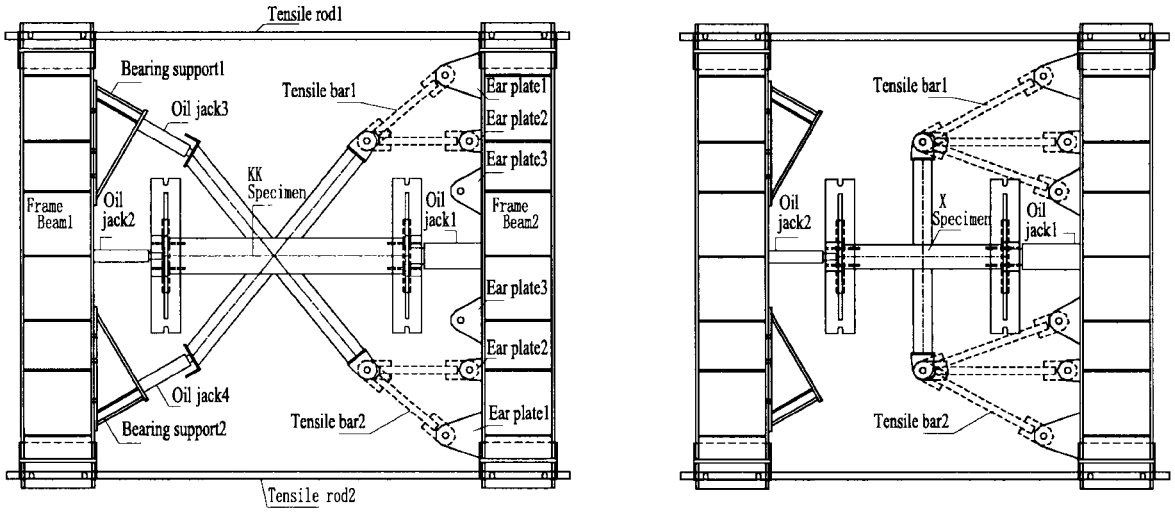

Fig. 3 Reaction frame and loading

Table 3 Overview of loading cases

Specimen	Loading case	N_{cr}/N_{cl}	e_1 (mm)	e_2 (mm)	N_{bt}/H_{bt}	N_{bc}/H_{bc}	N_{bc}/N_{bt}
DKL DKS	DKL-1 DKS-1	1: 0.2	50	100	1: 0.194	1: 0.384	1:1.538
	DKL-2 DKS-2	1: 0.2	-50	-100	1: 0.194	1: 0.384	1:1.538
	DKL-3 DKS-3	1: 0.2	0	0	1: 0.194	1: 0.384	1:1.538
	DKL-4 DKS-4	1: 0.63	0	0	1: 1.23	-	0:1.000
	DKL-5 DKS-5	1: 0.2	0	0	1: 1.23	1: 0.384	1:0.763
SXR SXN	SXR-1 SXN-1	-	0	0	-	-	-
	SXR-2 SXN-2	1: 0.625	0	0	1: 1.963	-	-
	SXR-3 SXN-3	1: 0.625	0	0	-	1: 2.747	-
	SXR-4 SXN-4	1: 0.4	0	0	0	0	-

Loads can be applied on the joint not only by the hydraulic jacks interposed between the frame beam or the bearing supports and the specimen but also by the rigid tensile bars connected with the ear plates. Such a loading-balance system is rather flexible. Various loading cases can be executed by changing the relative position of the jacks to the axis of the members, the combination of jacks with different capacities and the initial angle between the tensile bar and the axis of tensile brace of the test specimen.

The hydraulic jack 1, having 1000 kN loading capacity and the jack 2 to 4, having 200 kN capacity, are utilized in this test. In particular, the moments out of the plane of the chords-braces are applied by eccentric loads exerted by jack 1 and 2 on the ends of the chord.

By installing rollers under the frame and the specimen, the external load and inner forces in the horizontal are balanced within the system of frame-specimen. According to the balancing condition of the beam 1 and 2, the forces of the tensile rods and the bars can be respectively computed by the loads of jacks, that is to say, the inner forces of the specimen will be determined.

3.4. Loading cases

Five loading cases are programmed to each KK joint specimen to find if the combination of axial force and moment of the chord, the combination of axial force and shear force of the brace and the combination of different axial forces of the compressive and tensile braces affect the joint flexural behavior or not. The compressive braces are loaded directly by jack 3 and 4, and the tensile braces by rigid tensile bars. The loading directions and eccentricities, e_1 and e_2, as shown in Fig. 12, are regarded as positive.

Four loading cases are also programmed to each X joint specimen. The first case is the out-of-plane bending of the braces and end loads perpendicular to the chord-brace plane are applied to two brace members. The second is the combination of the compression and in-plane bending. The third is the

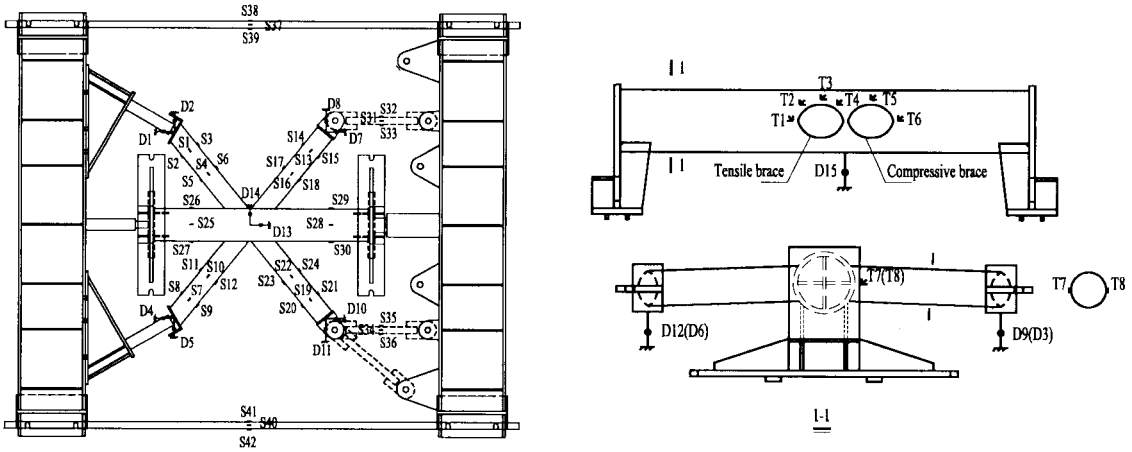

Fig. 4 Example of arrangement of measuring instruments

combination of the tension and in-plane bending. And the last case is the pure bending in-plane without axial forces applied on braces.

Table 3 gives the overview of all loading cases. In the table, N_{ct}, N_{cl}, e_1, e_2, N_{bt}, N_{bc}, H_{bt} and H_{bc} are defined in Notation at the end of this paper, with the subscript '*t*' to tensile brace and '*c*' to compressive one.

The maximum loads are limited in advance so that the specimen could be in elastic behaviors except for the last loading case. While the bending resistance is investigated in the last loading case of each specimen.

3.5. Measurements

The arrangement of the measuring instruments used in KK joint specimens is shown in Fig. 4. Among them, one-way strain gages (S1~S42) are used to check inner forces of members and tensile bars so as to monitor the loading processes, three-way strain gages (T1~T8) to learn about the complex stress distribution of the joint field, and displacement censors (D1~ D15) to survey the displacements along three orthogonal directions in the end of every brace member and in the midpoint of the chord.

4. Analytical model

The behavior of the unstiffened joint is dependent on the section size of the connecting members. When the wall becomes thin to some extent, the joint will take on a relative rotation at the intersection between the brace and the chord wall, which is caused by the bending moment. A model with limited constraint against rotation may account for this case very well. But on the other hand, when the wall is extremely thick, the length of the flexural deformation of the brace will be shortened, as can be seen in Fig. 5b, so that the joint can be characterized by a model with rigid field in the ends of the brace axis within the zone of the chord member.

Rigidly connected model(Fig. 5a), named here model A, intermediate between the upper two models,

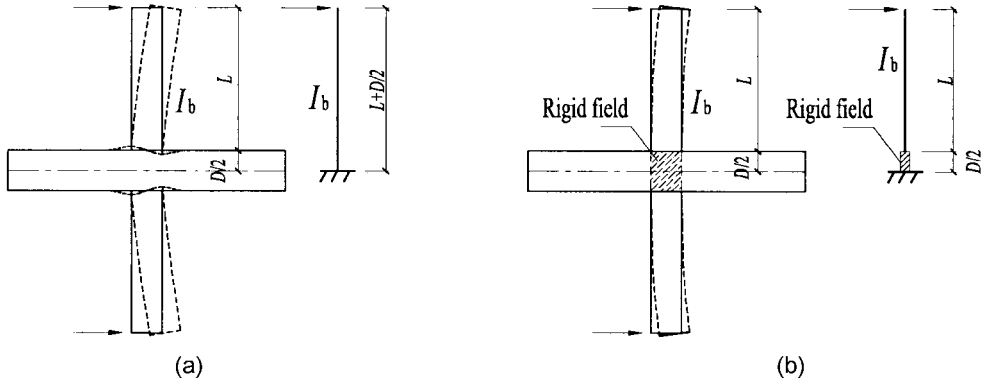

Fig. 5 Analytical model

and the rigid field model, named here model B, are used in the analysis of these four joint specimens. Model A is also what the engineers often used to analyze the structure both for its strength and stability. Though other analytical models can be constituted, the prediction by these two ideal models will cover the test data well as shown next.

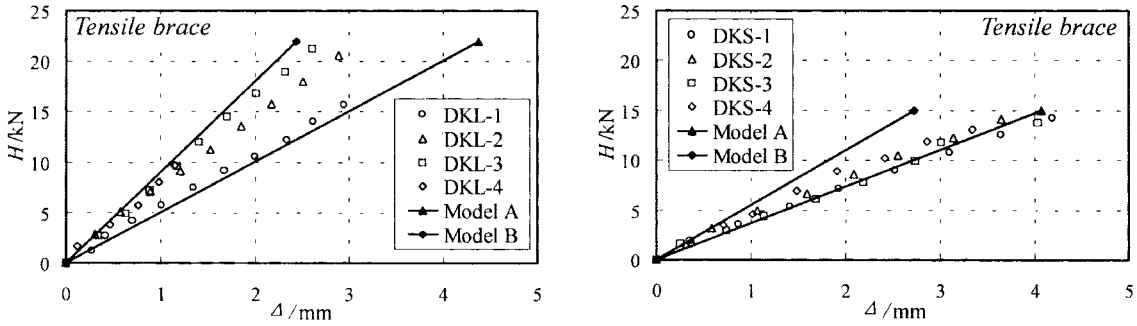

Fig. 6 Lateral force-elastic deflection curves of DKL and DKS

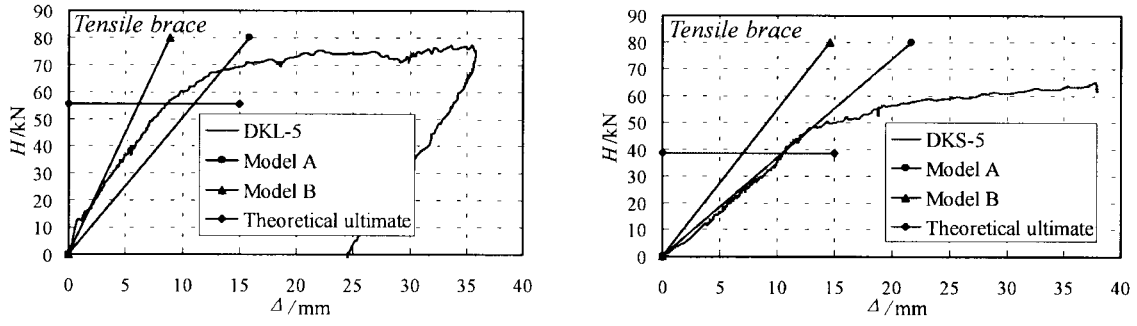

Fig. 7 Lateral force- elasto-plastic deflection curves of DKL and DKS

5. Experimental results and comparison with analytical model

Figs. 6 to 9 are part of the lateral force-deflection curves for the different specimens tested under various loading cases. Fig. 10 are the vertical force-deflection curves for SXN and SXR under their first loading cases. Where, vertical axis represents the lateral or vertical force at the brace end, H or Q, which is perpendicular to the axis of the brace, and horizontal axis represents the end displacement, Δ or ξ, correspondingly, which is gained by subtracting rigid body movement from the measured data at the ends of the braces. In each figure the lateral or vertical force-deflection curves of the analytical

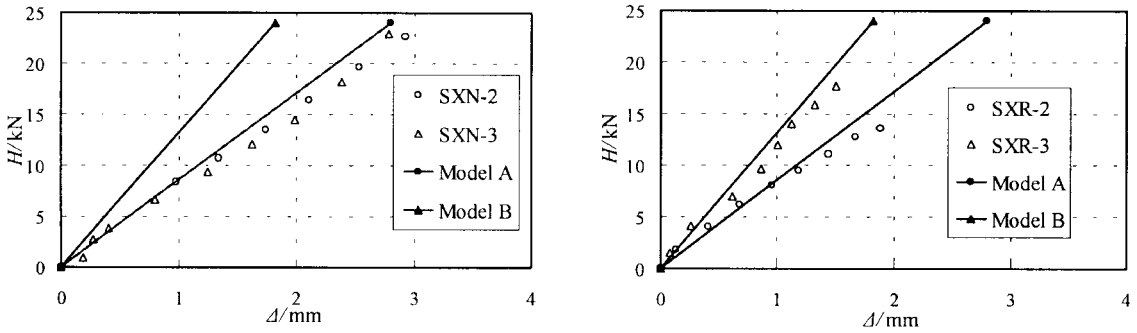

Fig. 8 Lateral force- elastic deflection curves of SXN and SXR

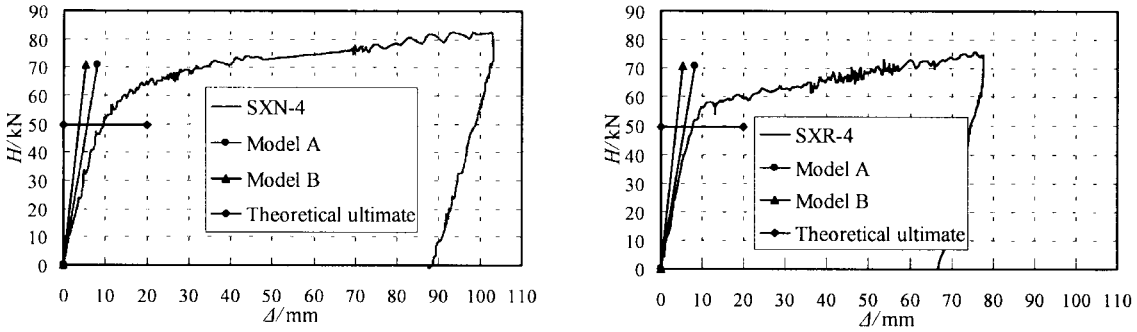

Fig. 9 Lateral force- elasto-plastic deflection curves of SXN and SXR

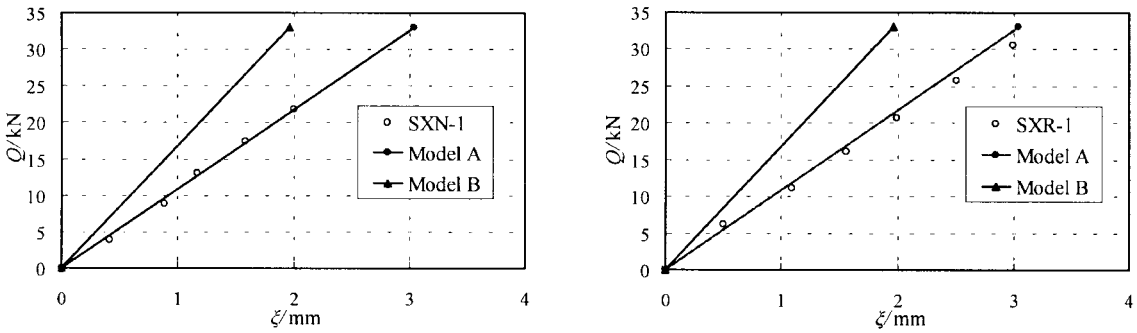

Fig. 10 Vertical force- elastic out-of-plane deflection curves of SXN and SXR

Table 4 Numerical comparison between analytical and test results for DK joints (kN/mm)

Loading case	Tensile brace			Compressive brace			Loading case	Tensile brace			Compressive brace		
	Test value	Model A	Model B	Test value	Model A	Model B		Test value	Model A	Model B	Test value	Model A	Model B
DKL-1	5.2			10.4			DKS-1	3.3			4.2		
DKL-2	6.9			10.5	6.1	10.9	DKS-2	3.8			4.3	4.5	6.6
DKL-3	8.3	5.0	9.0	11			DKS-3	3.5	3.8	5.5	4.1		
DKL-4	7.9						DKS-4	4.0					
DKL-5	8.0						DKS-5	3.6					

Table 5 Numerical comparison between analytical and test results for SX joints (kN/mm)

Loading case	Description of brace	Test value	Model A	Model B	Loading case	Description of brace	Test value	Model A	Model B
SXR-1	Out-of-plane bending	10.3	10.8	16.8	SXN-1	Out-of-plane bending	11.0	10.8	16.8
SXR-2	Tension and in-plane bending	7.1			SXN-2	Tension and in-plane bending	7.6		
SXR-3	Compression and in-plane bending	11.6	8.6	13.2	SXN-3	Compression and in-plane bending	7.8	8.6	13.2
SXR-4	In-plane bending	6.6			SXN-4	In-plane bending	6.2		

models mentioned in the last section are given. Shear deformation and second-order effect are neglected in the analytical results.

By the comparison of experimental results with theoretical models, the joint rigidity can be estimated. Furthermore, the greater the slope of the experimental curve in elastic range is, the more rigid the joint is. The slope value (or initial stiffness) of the elastic curves for different types of joint examined are listed in Table 4 and Table 5 respectively. Where, the test value is the average of the two symmetrical braces.

5.1. Elastic flexural behavior

From Figs. 6, 7 and Table 4 it emerges that the initial stiffness of the joints DKL and DKS are almost within the range that model A and B predict. For DKL, test values of tensile braces lie between initial stiffness of model A and B, and test values of compressive braces are close to that of model B. For DKS, test values are a little smaller than DKL. But according to the classification of connections in Eurocode for steel frame structures, DKS can be considered as rigid joint. The similar fact is also observed to the joins SXR and SXN from Fig. 8 to Fig. 10 and Table 5. On the whole, the results indicate that tested unstiffened tubular joints have local flexural rigidity high enough to be supposed as rigidly connected in the given conditions.

The magnitude and the state of axial force, tension or compression, as well as the loading conditions of the neighboring members have influence on the flexural behavior of tubular joint. From Table 4, strong evidences that joint zone under the compressive brace develops an obvious rigid behavior can be seen. This phenomenon may be explained by that the relative rotation at the intersection between the

chord wall and compressive brace are counteracted because of the bigger absolute axial value of tensile brace than that of compressive brace. By contrast of the fourth case with the other cases of KK joints, we can find that the neighboring compressive brace is contributing to the relative rotational deformation of tensile brace.

By scaling Fig. 8 and Fig. 10, it can be read that the ratio of the out-of-plane deflection tested to that of model A is 110%, while the in-plane deflection tested is 130 percent of that of model A. It demonstrates the difference of rotational constraint applied to the braces between both directions.

5.2. Factors affecting the joint flexural behavior

The flexural behavior of the joint is attributed to the interactive effects of following principal factors, by observation from the tests:

- Geometrical characteristics

Geometrical parameters of the member section, namely β (d/D), γ ($D/2T$), and τ (t/T), play an important role in the flexural behavior of the joint. Among them, for any two given geometry, joint rigidity increases with the other parameter decreasing. In other words, to enhance the chord will provide the brace more solid constraint base.

- Initial included angle between chord and brace

If other factors remain same, the smaller angular degree leads to more rigid joint behavior due to the increase of the intersection area of chord and brace. The comparison of DKS with SXN is a good case for this point.

- Stiffener

Though little difference can be found for SXR and SXN in elastic stiffness with braces tensioned or no axial loaded from Fig. 8 and Fig. 9, the elastic stiffness of SXR with braces compressed and its postyielding stiffness are higher than that of SXN.

5.3. Failure modes

Failure modes of all these specimens are described in Table 6. On the whole, failure modes of them can be classified into brace yielding type, though slight local plastic deformation of the chord occurred in the joint zone.

Table 6 Failure modes of joint specimens

Specimen	Description		
	Brace	Chord	Welds
DKL	Slight residual flexural deformation in tensile brace and local buckling on the compression side at the tensile brace end	No observable convex and concave wall deformation	No cracking
DKS	Obvious residual flexural deformation in tensile brace, oval section at the tensile brace end and slight flexural deformation in compressive brace	Same to DKL	No cracking
SXR	Obvious residual flexural deformation and elasto-plastic local buckling on the compression side at the brace end	Slight plastic deformation in the joint zone	No cracking
SXN	Obvious residual flexural deformation in tensile brace and ovalized section at the brace end	Same to SXR	No cracking

5.4. Bending resistance

According to the ultimate analysis considering the effect of axial loads, *N-M* correlation for circular tube section deduced by Chen (1976) is put forward as follows:

$$\begin{aligned} 0 \leq N/N_p \leq 0.65 \quad & M/M_p = 1-1.18\ (N/N_p)^2 \\ 0.65 \leq N/N_p \leq 1 \quad & M/M_p = 1.43\ (1-N/N_p) \end{aligned} \tag{1}$$

Where, N_p, M_p, refer to the plastic axial load and plastic moment.

The dimensionless axial force N/N_p is 0.04 for DKL and 0.034 for DKS, respectively, when the brace end section yields, while zero for SXR and SXN. Theoretical ultimate calculated through Eq. (1) are plotted in a straight line in Fig. 7 and Fig. 9. It can be noticed that the test values corresponding to brace yielding and the predicted values show good agreement for KK and X specimens.

Test results clearly demonstrate that the initial stiffness of the curves can be maintained by the joint rigidity until theoretical ultimate is reached. In other words, the bending capacities of unstiffened joints can assure the strength of the members connected under certain limitation of geometrical parameters.

5.5. Postyielding flexural behavior

After yielding, the stiffness of the brace decreases drastically and strain-hardening behavior is observed up to the end of loading. No evidence about the dramatic loss of bearing capacity is obtained in the performed tests. The ratio of the postyielding stiffness to the elastic stiffness for these four joints are determined from the elasto-plastic curves to be 0.13(DKL), 0.08(DKS), 0.05(SXR) and 0.035(SXN) respectively. This signifies that the effect of the geometrical parameters on postyielding stiffness bears a resemblance to that on elastic stiffness.

6. Finite element validation

6.1. Numerical procedure

The purpose of the finite element analyses is to extend the interpretation of the results and observations obtained in the tests, to gain a better understanding of the flexural behaviour of tubular joints. The first stage of any FE study which aims to this purpose is necessarily the validation of the strategy against reliable test results to ensure that, as far as possible, the actual joint behaviour can be well simulated. The strategy used must reliably reproduces the overall load-deformation behaviour and model the failure modes. For the sake of it, the classical theory of thin shells and the techniques of the finite element method are combined.

Four test joints are selected for validation. Geometrical details of them are given in Section 3.2. Eight-noded, three-dimentional structural shell elements are used throughout the models except for the steel tensile bars, which are modeled using 3-D beam element. The shell element, having six degrees of freedom at each node: translations in the nodal *x*, *y*, and *z* directions and rotations about the nodal *x*, *y*, and *z* axis, is particularly well suited to model curved shells. Its deformation shapes are quadratic in both in-plane directions. The connection between the shell element and the beam element is achieved by the coupling of nodal DOFs.

A study is carried out to determine the reasonable mesh density in terms of computation time and

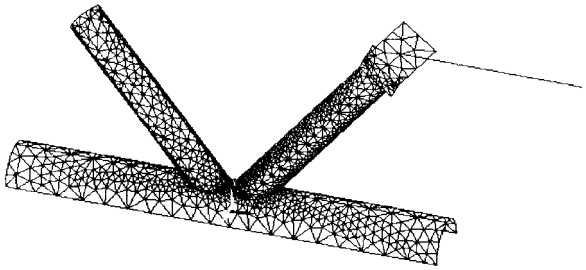

Fig. 11 FE model of the joint DKL

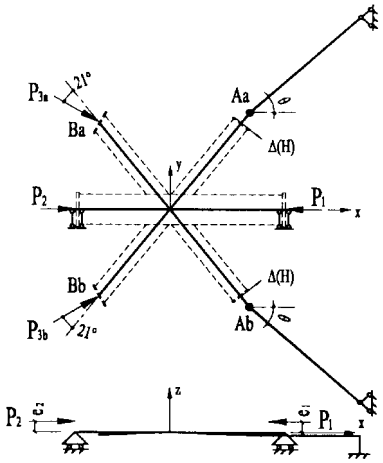

Fig. 12 Loading and boundary conditions

accuracy, by varying the number of elements used for the model. Note that the maximum thickness to length(or width) ratio is 0.2 for all elements including those situated near the geometrical discontinuity. The mesh used here is relatively coarse to allow a quick turnover of analysis, but is adequate to model the main features of the force-deflection responses to the loading cases.

The FE model of the joint DKL used in the present work is shown in Fig. 11. The global coordinate system is a rectangular Cartesian (XYZ) system. The boundary restrains applied, Fig. 12, simulate those used in the tests. Due to symmetry and loads, only one-half of the joint is modeled explicitly, with symmetry boundary conditions being applied along the plane of symmetry.

The general-purpose nonlinear FE package program ANSYS (ANSYS 1998) is employed for the analyses. The analyses include geometric and material non-linearity effects, due to the large displacements of the chord wall during deformation and the elastic-plastic behaviour of the material during failure. The materials are assumed to obey the Von Mises yield criterion and the associated Prandtl-Reuss flow rule. Young's modulus of the material is taken as 206 kN/mm^2 and Poisson's ratio as 0.3. The material laws are modeled by a piecewise linear representation of the stress-strain curves. The analyses are both incremental and iterative and the modified Newton-Raphson solution algorithm is used.

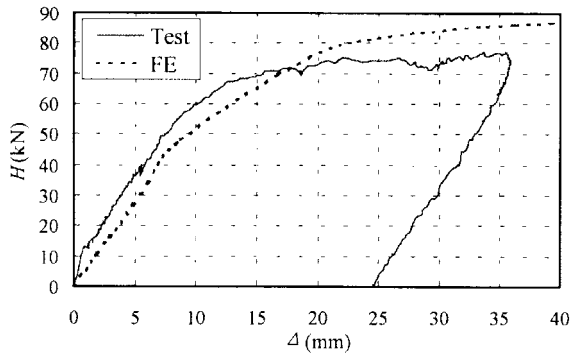

Fig. 13 Load-displacement results for joint DKL

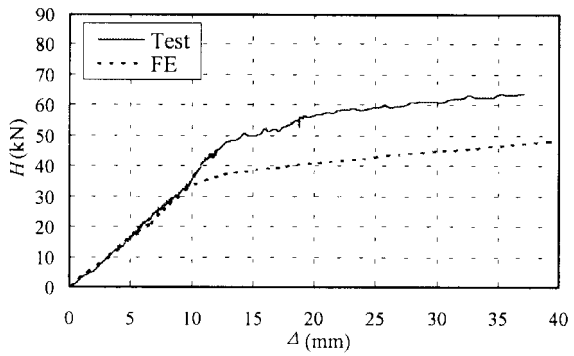

Fig. 14 Load-displacement results for joint DKS

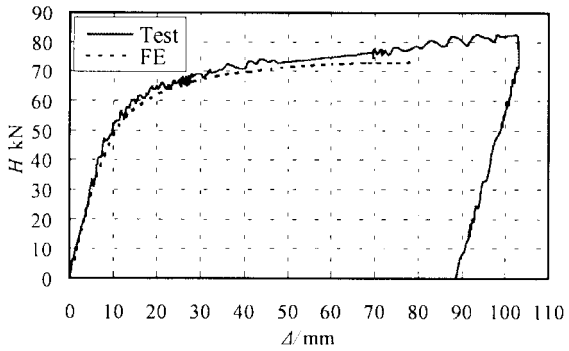

Fig. 15 Load-displacement results for joint SXN

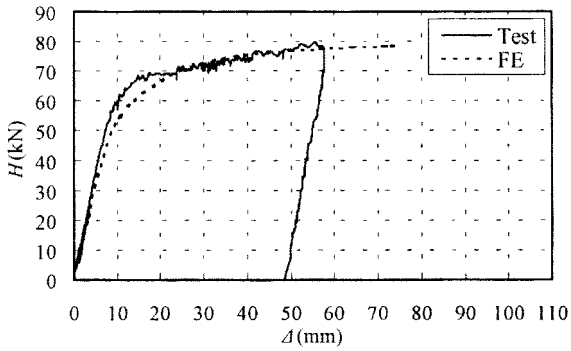

Fig. 16 Load-displacement results for joint SXR

6.2. Verification of FE model

The load-displacement curves obtained from the FE calculations are compared with the experimental curves. The curves, both FE and experimental, are obtained using the lateral force at the end of the brace and corresponding deflection. The models are created to the mid-surface dimensions of the test joints. It can be seen that the FE model captures the flexural behavior in a satisfactory way. The initial stiffness and postyielding stiffness agree with that of the test joint well, however, the ultimate load is some different for DKL and DKS. This disparity is due probably to no weld modeling. Though no weld effect is considered in the conducted FE analysis, it is indicated that weld modeling may not be important for the investigation of flexural deformability of tubular joints (Dexter *et al.* 1996). Furthermore, the test joint failed with the phenomenon of local buckling at brace end, which can be seen in Fig. 17a, is well simulated by the FE model analysis, referring to the deformed mesh in Fig. 17b.

The excellent correlation obtained between the numerical and the test results intimates that the FE strategy developed is valid and accurate, especially for the assessment of the joint stiffness. The strategy is then used to develop the parametric formula for local rigidity of T and Y type tubular joints in next section.

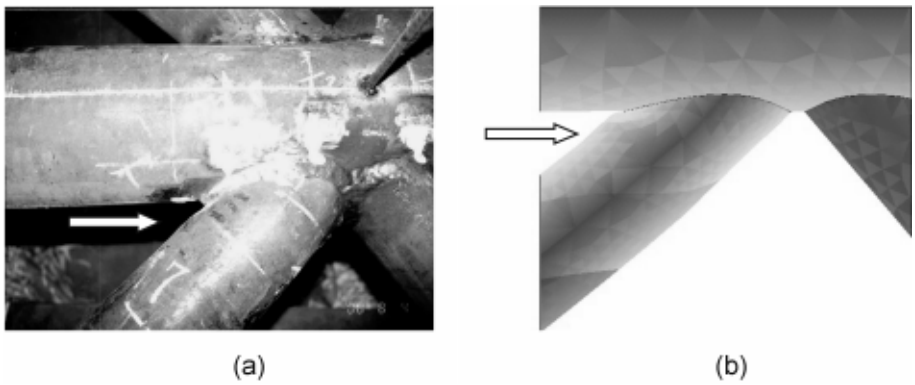

Fig. 17 Comparison of failure modes for joint DKL

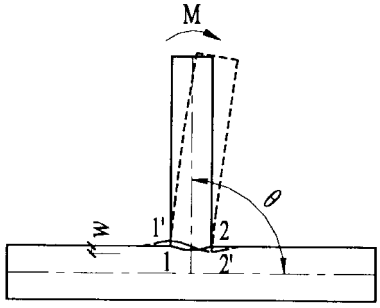

Fig. 18 Local deformation of T joint

7. Parametric formula for local inplane bending rigidity of T and Y tubular joints

7.1. Definition

The local joint bending rigidity of tubular joints, K_M, can be defined as the ratio of the brace-end moment to the rotation due to the local deformation of chord wall. In this paper, however, only the inplane rigidity is discussed.

For T and Y joints (Fig. 18),

$$K_M = M/\phi \tag{2}$$

where M denotes the inplane bending moments at the brace end section adjacent to chord wall, and ϕ denotes the local inplane rotation at the same point, which is caused by M.

In practical calculation, the reference points located on the intersection of the brace and the chord wall are chosen. As shown in Fig. 18, the deformation at point 1 and 2, denoted as w_1 and w_2, is the local wall convex or concave, exclusive of the global deformation of the connected members. Thus the total inplane rotation at the reference points is computed as follows:

$$\phi = \frac{w_1 - w_2}{d - t}\sin\theta \tag{3}$$

and

$$K_M = M\,(d–t) / [(w_1 - w_2)\sin\theta] \tag{4}$$

where θ is the angle between the brace and the chord, d and t are the brace diameter and thickness respectively.

7.2. Parametric formulae

For the convience of practical design, a parametric formula for evaluating the inplane bending rigidity of the planar T and Y tubular joints is proposed by the authors, which is formulated through regression of the data from the FE analyses.

$$K_M = 0.362ED^3(\sin\theta)^{-1.47}\gamma^{-1.79}\tau^{-0.08}\beta^{2.29} \tag{5}$$

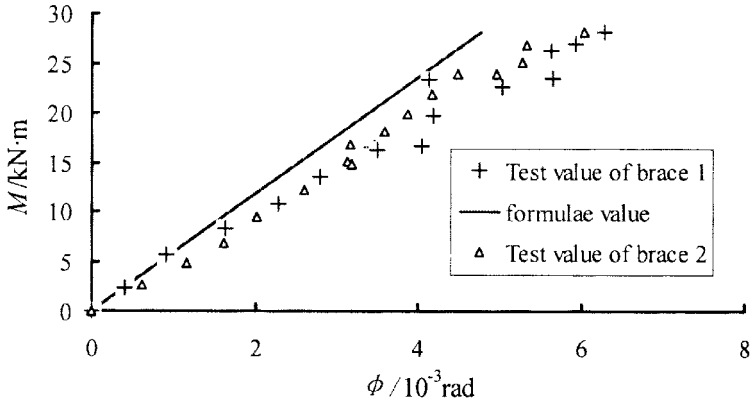

Fig. 19 Comparison of formulae with test value

The above formula is valid for tubular joints with geometric parameters $\beta = 0.2\text{-}1.0$, $\gamma = 10\text{-}50$, $\tau = 0.2\text{-}1.0$ and $\theta = 30^{\circ}\text{-}90^{\circ}$.

7.3. Comparision with test results

The value of the bending rigidities given by the parametric formula (5) is compared with the test data from joint specimen SXN. The comparison is shown graphically in Fig. 19. It may be seen that the parametric formula generally provide a good fit to the test results. It can be concluded that the formula is reliable on the whole in evaluating the local rigidity of tubular joints and can be recommended in use in the global structural analysis of steel-tube structures.

The evaluation of the bending rigidity of K joint on Uni-KK joint will definitely relate to the local axial deformation and the influence of the two braces, and more parameters should be taken into account. The expression of the joint rigidity will be more complex. Limited by the pages, the contents will be introduced in other reports.

8. Conclusions

Two uni-planar KK unstiffened tubular joints and two X tubular joints are tested under several loading combinations respectively. Analytical models are established to make a comparative base for rigidity estimation. FE strategies for modeling tubular joints are verified against test data. Failure modes can be accurately reproduced. A parametric formula for local rigidity of T and Y joints is proposed on the basis of FE calculation and regression analysis.

Based upon the experimental behavior of joints and theoretical analyses, the following conclusions have been reached:

(1) The bending rigidity is largely dependent on the geometrical parameters of the joint. The unstiffened joints can be referred as full rigid joints, and their bending capacities can assure the strength of the members connected under certain limitation.

(2) It will be necessary to establish sufficient tubular connection deformation data for the development of parametric formulae giving the rigidity associated with various connection. The

data of connection rigidity reported in this paper represent a contribution to this endeavour.

(3) The FE strategies developed here can be used to carry out a parametric study on unstiffened tubular joints.

(4) Parametric formula for local rigidity of T and Y tubular joints developed in this paper has good applicability, and this work lays a foundation for providing a clear criteria to classify the unstiffened tubular joint.

Reference

ANSYS (1998), *ANSYS Users Manual Revision 5.5*, ANSYS, Inc., Canonsburg, Pennsylvania.

Bouwkamp, J.G. et al. (1980), "Effect of joint flexibility on the response of offshore structures", *In Proc Offshore Technol Conf. Houston,* TX.

Chen, W.F., Atsuta, T. (1976), *Theory of Beam-Columns, Vol. 1: In-Plane Behavior and Design,* McGraw-Hill, New York.

Dexter, E.M., Lee, M.M.K., Kirkwood, M.G. (1996), "Overlapped K joints in circular hollow sections under axial loading", *Journal of Offshore Mechanics and Arctic Engineering,* **118**(2), 53-61.

Fessler, H., Spooner, H. (1981), "Experimental determination of stiffness of tubular joints", *Proc. 2nd Int. Symp. on Integrity of Offshore Structures,* Glasgow.

Gibstein, M.B. (1987), "Stress concentration in tubular K-joints with diameter ratio equal to one", *Steel in Marine Structures,* Elsevier Science Publishers B. V. Amsterdam.

Holmas, T. (1987), "Implementation of tubular joint flexibility in global frame analysis", *Report No. 87-1 Division of structural mechanics,* The Norwegian Institute of Technology.

Kurobane, Y., Makino, Y. and Ochi, K. (1984), "Ultimate resistance of unstiffened tubular joints", *J. Struct. Eng.,* ASCE **110**, 385-400.

Moffat, D.G., Mwenifumbo, J.A.M., Xu, S.H., et al. (1991), "Effective stress factors for piping branch junctions due to internal pressure and external moment loads", *Journal of Strain Analysis,* **26**, 85-101.

Ogawa, K., Makino, Y., Yamanari, M. and Kurobane, Y. (1987), "Effective length for web members in tubular truss", *Journal of Struct. Const. Engrg., Transaction of AIJ*, No. 388

Packer, J.A. and Henderson, J.E. (1992), *Design Guide for Hollow Structural Section Connections*, Canadion Institute of Steel Construction, 38~47.

Rodabaugh, E.C. (1980), "Review of data relevant to the design of tubular joints for use in fixed offshore platforms", W.R.C.

Rondal, J. (1990), "Effective lengths of tubular lattice girder members", *CIDECT Report*, 3K-90/3.

Soh, A.K., Soh, C.K. (1993), "Hot Spot stress of K tubular joints subjected to combined loadings", *J. Const. Steel Research,* **26**, 125-140.

Szlendak, J., Brodka, J. (1985), "Strengthening of T moment of RHS joints", *Proc. Instn Civ. Engrs,* Part 2, **79**, 717-727.

Ure, A., Grundy, P., et al. (1993), "Flexibility coefficients of tubular connections", *Tubular Structures,* London.

Wang, W., Chen, Y.Y., Chen, Y.J., Zhao, X.Z. and Liu, P. (2001), "Experimental research on flexible rigidity of uni-planar KK tubular joints", *Proceedings of 6th Pacific Structural Steel Conference,* Beijing, October.

Wardenier, J., Kurobane, Y., Packer, J.A., Dutta, D. and Yeomans, N. (1991), *Design Guide for Circular Hollow Section (CHS) Joints under Predominantly Static Loading,* Verlag TUV Rheinland, Koln.

Yura, J.A., Zettlemoyer, N., Edwards, I.F. (1981), "Ultimate capacity of circular tubular joints", *J. Struct. Eng.,* ASCE **107**, 1965-1983.

Notation

N_{cr} compression applied to chord right to joint zone
N_{cl} compression applied to chord left to joint zone
N_{bt} axial force of tensile brace
H_{bt} shear force of tensile brace
N_{bc} axial force of compressive brace
H_{bc} shear force of compressive brace
e_1 out-of-plane eccentricity of loading on the right end of chord
e_2 out-of-plane eccentricity of loading on the left end of chord
β brace diameter to chord diameter ratio (d/D)
γ chord radius to chord wall thickness ratio ($D/2T$)
τ brace wall thickness to chord wall thickness ratio (t/T)

CC